Finite-element simulation of HTS bulk reluctance motor

Xu Z., Qiu M., Yao Z.H., Xia D.

Institute of Electrical Engineering, Chinese Academy of Sciences, Beijing 100080, P.R. China

A Demo HTS reluctance motor with the rotor containing bulk YBCO elements is presented. Based on YBCO bulk magnetic characteristics, the field distribution in the motor and the resulting torque are evaluated by finite-element analysis. The feasibility of our method is proved by comparisons with the simulation and the following experiment.

INTRODUCTION

The development of HTS materials, both tape and bulk, has allowed the design of systems in several areas of electro-mechanical engineering. In particular, YBCO bulks have been used directly in electrical motors, such as hysteresis motors. It is expected that these novel motors possess higher output power, efficiency and power factor than the conventional ones [1]. For simplicity, HTS bulks are usually regarded as a material with constant permeability in the design. However, HTS bulks show strongly anisotropic and non-linear behaviors in magnetic fields. Based on the critical model, the finite-element method is presented to analyze a small Demo HTS reluctance motor in the paper. Its feasibility is proved by the experiments.

SPECIFICATIONS OF DEMO RELUCTANCE MOTOR

A two-pole, three-phase HTS demo reluctance motor has been developed in IEE/CAS. The technical parameters and basic structure are shown in Figure 1. Here P_2 is the output power, $U_{N\varphi}$ is the phase voltage (Y-connection), I_N is the phase current, f_1 is the frequency, D_{i1} is the inner diameter of the stator, l_{ef} is the effective length of the rotor, σ is the gap length. The difference from the conventional one is that the motor uses YBCO bulks instead of aluminum or air filled in the slots of the rotor.

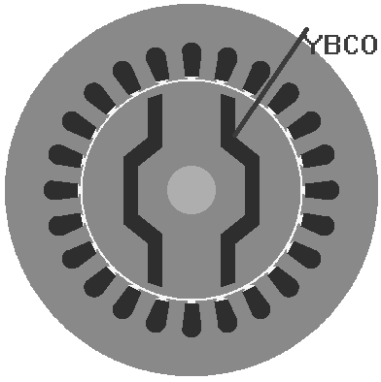

Figure 1 Cross section of the HTS reluctance motor

FINITE-ELEMENT ANALYTICAL METHOD

The operation of HTS bulk reluctance motor depends on the direct-axis (*d*-axis) synchronous reactance X_d, the quadrature-axis (*q*-axis) synchronous reactance X_q and the phase resistance of the stator winding R. In order to evaluate its operating characteristics, it is necessary to obtain values of X_d and X_q, by solving the field distribution in the motor firstly. For the demo motor, its length is much greater than its radius. The analytical model can be two-dimensional by neglecting end-effects. It is assumed that the motor operates in synchronous regime and no fundamental eddy current would be induced in the rotor. So the inner magnetic field can be approximately treated as stationary. HTS bulks are treated as nonlinear magnetic mediums rather than idealized conducting materials. Magnetic qualities of YBCO bulk is defined by the magnetization curve [4].

The field distribution in the cross section of the motor is calculated in a rectangular coordinate system, with the *x*-axis parallel to the *q*-axis of the rotor and the *y*-axis parallel to the *d*-axis. Considering the non-linearity of silicon-steel and the anisotropy of YBCO, the two-dimensional quasi-Poisson's equation is adopted to describe the mathematical model of the magnetic field in the cross-section:

$$\frac{\partial}{\partial x}(v_{\mathrm{y}}\frac{\partial \boldsymbol{A}}{\partial x})+\frac{\partial}{\partial y}(v_{\mathrm{x}}\frac{\partial \boldsymbol{A}}{\partial y})=-\boldsymbol{J} \qquad \text{in the section area of the motor} \tag{1a}$$

$$\boldsymbol{A}=0 \qquad \text{on the outside border of the section area} \tag{1b}$$

where $\boldsymbol{A}$ is the magnetic vector potential; v_x, v_y are the x-axis and y-axis reluctivity at arbitrary point in the cross section; and $\boldsymbol{J}$ is the source current density. When solving Equation (1) by finite-element method, local *B*-*H* curves of each finite element is calculated by expression (2) and then assigned as a property to that finite element.

$$\boldsymbol{B}(\boldsymbol{H})=\mu_0[\boldsymbol{H}+\boldsymbol{M}(\boldsymbol{H})] \tag{2}$$

where $\boldsymbol{B}$ is magnetic flux density, $\boldsymbol{H}$ is magnetic field intensity, $\boldsymbol{M}$ is magnetization vector and μ_0 is free space permeability. local M (H) data of each YBCO finite element is achieved from the expressions given in [5], which is based on the Kim model of the Type-Ⅱ superconductors. Some parameters are corrected by our experimental measurements. After the field distribution is worked out, X_d and X_q can be computed exactly. Subsequently, the operating characteristics of the motor can be evaluated easily.

RESULTS AND DISSCUSSIONS

Figure 2 shows the distribution of the magnetic field under θ=0° and θ=90° after rated current is injected into the stator winding, where θ is the angle between the rotary magneto-motive potential vector and the d-axis of the rotor. Thereout, the radial air-gap induction B_r is computed by the following expression:

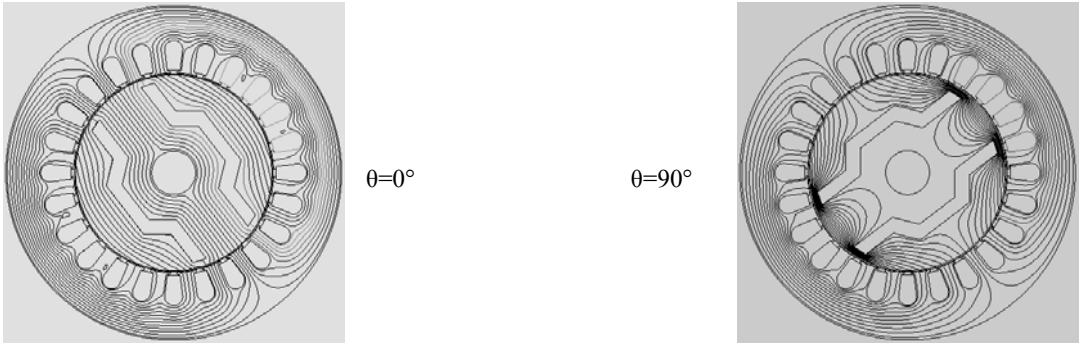

Figure 2 Magnetic flux distribution within the motor

$$B_r = \boldsymbol{B} \bullet \boldsymbol{R^0} = (\frac{\partial \boldsymbol{A}}{\partial y}\boldsymbol{i} - \frac{\partial \boldsymbol{A}}{\partial x}\boldsymbol{j}) \bullet (x_r \boldsymbol{i} + y_r \boldsymbol{j}) / \sqrt{x_r^2 + y_r^2} \tag{3}$$

where (x_r, y_r) is the coordinate of arbitrary point at the circle line in the gap. The fundamental component of B_r can be obtained further by Fourier decomposition. The B_r after ABS transform is shown in Figure 3. It can be seen that YBCO bulks have obviously blocked the fluxes in the direction of q-axis.

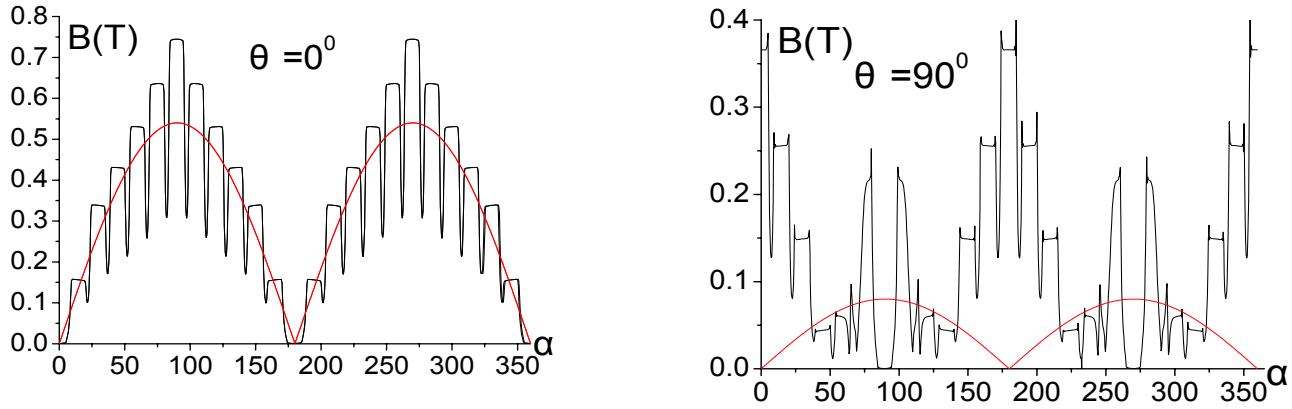

Figure 3 Radial air-gap induction within the motor

It's supposed that $i_A=I_m$, $i_B=-0.5I_m$, $i_C=-0.5I_m$ and $\theta_0=0$ at a particular time. Here i_A, i_B, i_C are stator phase currents with the amplitude of I_m, θ_0 is the angle between the d-axis of the rotor and the axis of A phase winding. In terms of the definition of the direct-axis synchronous reactance, X_d can be expressed as:

$$X_d = 2\pi\pi \frac{\sum_{k=1}^{N} \iint_S \boldsymbol{B} \bullet \boldsymbol{ds}}{a I_m / \sqrt{2}} \tag{4}$$

where S is the area of the single turn coil, a is the number of parallel branches of stator winding, f is the frequency of stator fundamental current, and N is the number of total turns of the single-phase winding. Likewise, X_q may also be determined as shown in Figure 4. It can be seen that both X_d and X_q decline with the increase of their respective exciting currents. Also, we find the X_q-I_q curve drops rapidly when I_q is lower than 0.45 A. All these observations from Figure 4 are in accordance with the experimental data, which proves the validity of the analytical method we presented above.

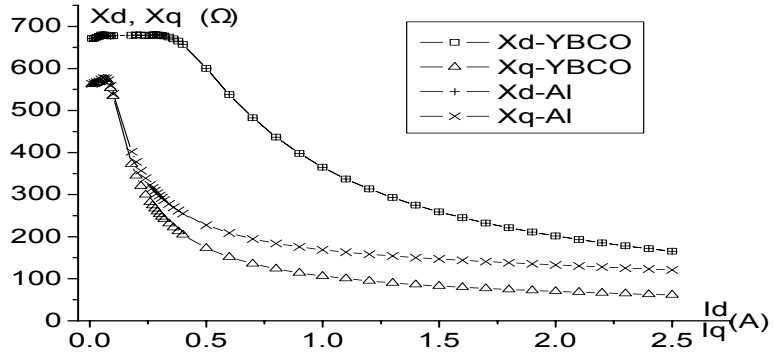

Figure 4 X_d-I_d and X_q-I_q curves of the motor

Based on curves of X_d- I_d and X_q- I_q, the working curves of the HTS reluctance motor can be completely determined by the electrical machine theory, as shown in Figure 5. In the figure, P_2 is the output power, T is the output torque, I is the stator current, cosφ is the power factor, η is the efficiency and θ is the power angle. The corresponding experimental results are shown in Table 1. The comparison reveals the

feasibility of our finite-element analytical method.

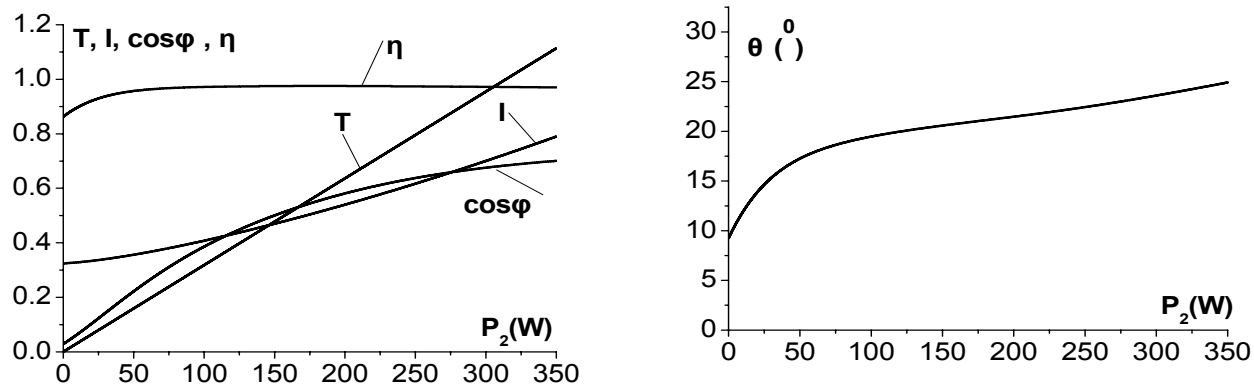

Figure 5 Working curves of HTS bulk reluctance motor

Table 1 The comparisons of the computational and experimental data (220V)

	P_2 (W)	I (A)	cos ϕ	η
Experimental value	150	0.50	0.49	0.948
computation value	150	0.47	0.50	0.975
Experimental value	300	0.72	0.70	0.907
computation value	300	0.70	0.68	0.972

CONCLUSION

Considering that the strongly anisotropic and non-linear magnetic behaviors of HTS bulk, a finite-element method is presented to analyze a small Demo HTS reluctance motor. Its feasibility is proved by the comparisons between the experimental and simulated results of X_d- I_d, X_q- I_q curves and the operating characteristics.

ACKNOWLEDGMENT

The work was supported by the National Nature Science Foundation of China under Grant No. 50107010.

REFERENCES

1. Kovalev L. K., Oswald B., Gawalek W., Superconducting Reluctance Motor with YBCO Bulk Materials, IEEE Transactions on Applied Superconductivity (1999) 9 1201-1204

2. Kovalev L. K., Gawalek W., Oswald B., Hysteresis and Reluctance Electrical Machines with the Bulk HTS Rotor Elements, IEEE Transactions on Applied Superconductivity (1999) 9 1261-1263

3. Kovalev L. K., Gawalek W., Oswald B., New types of electric machines on the basis of the bulk HTS elements, Proc. of ICEC-18, Bornbay, India, (2000)

4. Vajda I., Mohacsi L., Advanced hysteresis model for levitating applications of HTSC materials, IEEE Transactions on Applied Superconductivity, (1997) 7 916-919

5. Chen D. X., Goldfarb R. B., Kim model for magnetization of type-II superconductors, Journal of Applied Physics (1989), 66 2489-2500